N-Terminal Sequences Direct the Autophosphorylation States of the FER Tyrosine Kinases in Vivo†

Kira Orlovsky, Israel Ben-Dor, Smadar Priel-Halachmi, Hana Malovany, and Uri Nir*

Faculty of Life Sciences, Bar-Ilan University, Ramat-Gan 52900, Israel

Received March 6, 2000; Revised Manuscript Received June 12, 2000

ABSTRACT: p94^{fer} and p51^{ferT} are two tyrosine kinases which share identical SH2 and kinase domains but differ in their N-terminal regions. While p94^{fer} is expressed in most mammalian cells, the accumulation of p51^{ferT} is restricted to meiotic spermatocytes. Here we show that the different N-terminal tails of p94^{fer} and p51^{ferT} direct different autophosphorylation states of these two kinases in vivo. N-terminal coiled-coil domains cooperated to drive the oligomerization and autophosphorylation in trans of p94^{fer}. Moreover, the ectopically expressed N-terminal tail of p94^{fer} could act as a dominant negative mutant and associated with the endogenous p94^{fer} protein in CHO cells. This increased significantly the percentage of cells residing in the G0/G1 phase, thus suggesting a role for p94^{fer} in the regulation of G1 progression. Unlike p94^{fer}, overexpressed p51^{ferT} was not autophosphorylated in COS1 cells. However, removal of the unique N-terminal 43 aa of p51^{ferT} or the replacement of this region by a parallel segment from p94^{fer} endowed the modified p51^{ferT} with the ability to autophosphorylate. The unique N-terminal sequences of p51^{ferT} thus interfere with its ability to autophosphorylate in vivo. These experiments indicate that the N-terminal sequences of the FER tyrosine kinases direct their different cellular autophosphorylation states, thereby dictating their different cellular functions.

p94^{fer} is an evolutionarily conserved (*1, 2*) nonreceptor tyrosine kinase encoded by the FER locus in human (*3*), mouse (*4*), rat (*5*), and *Drosophila* (*2*). The expression of p94^{fer} is widespread, and it is found in most mammalian cells (*3, 5*), though it was not detected in immune cells such as pre-B, pre-T, and T cells (*3*). p94^{fer} is structurally similar to the proto-oncogene c-Fes (*6*).

A truncated form of p94^{fer}, termed p51^{ferT}, is encoded by a testis-specific FER transcript. This tyrosine kinase was shown to accumulate in the nucleus of meiotic pachytene spermatocytes (*4, 7, 8*).

p94^{fer} and p51^{ferT} share common SH2 and kinase domains (Figures 1 and 3−5); the kinase domain is 70% homologous to the kinase domain of c-Fes (*6, 9, 10*). The two FER kinases differ, however, in their N-terminal regions [Figure 1 and (*3, 4*)]. While p94^{fer} carries a 412 aa tail in which 3 potential coiled-coil (CC)[1]-forming domains were identified (*11, 12*), in p51^{ferT} these N-terminal 412 aa are replaced via differential splicing, by a novel 43 aa long N-terminal tail (*4*). The N-terminal coiled-coil domains of p94^{fer} have been implicated in directing the subcellular localization (*11*) and oligomerization (*13*) of this kinase. A similar role of N-terminal coiled-coil sequences was demonstrated in the oligomerization of c-Fes (*14*). By analogy with the receptor PTKs (*15*), oligomerization of p94^{fer} and c-Fes (*14*) may potentiate their autophosphorylation in trans, and their subsequent activation in vivo.

The two FER kinases also differ in their subcellular distribution profiles. While the meiotic FER tyrosine kinase p51^{ferT} accumulates constitutively in the nucleus, and is not detected in the cytoplasm (*8, 11*), p94^{fer} is mainly cytoplasmic, though it enters the nucleus upon transition of cells from G1 to the S phase (*11*). In the cytoplasm, p94^{fer} associates with cell−cell adhesion molecules (*12, 16*), and its activity is induced in growth factor-stimulated cells (*12*). Moreover, p94^{fer} was shown to associate with activated EGF and PDGF receptors in fibroblasts (*12*) and with the FcϵRI receptor in mast cells (*17*). These findings suggest the involvement of p94^{fer} in growth-promoting pathways, though its involvement in such processes has not been proven directly.

To further understand the regulation of the FER kinases activity in vivo, and to establish new tools for analyzing their cellular functions, we have studied the role of their different N-terminal regions in modulating the autophosphorylation states of these kinases in vivo. Specifically we addressed the question whether oligomerization leads to autophosphorylation in-trans of the p94^{fer} kinase in vivo. Here we show that the N-terminal tail of p94^{fer} drives the oligomerization and the autophosphorylation of p94^{fer} in-trans, in vivo. Moreover, the independently overexpressed N-terminal tail can act in a dominant negative manner, interfering with the activation of p94^{fer} in vivo. Unlike p94^{fer}, the N-terminal tail of p51^{ferT} did not seem to support the autophosphorylation of this enzyme, but rather interfered with the autophosphorylation process. The different N-terminal tails of the FER

† This study was supported by a grant from the Israeli Cancer Research Foundation.

* Correspondence should be addressed to this author at the Faculty of Life Sciences, Bar-Ilan University, Ramat-Gan 52900, Israel. Phone: 972-3-5318757, Fax: 972-3-5351824, E-mail: nir@mail.biu.ac.il.

[1] Abbreviations: CC, coiled-coil; HA, influenza hemaglutinin; FCS, fetal calf serum; EIES, ecdysone-inducible expression system.

10.1021/bi0005153 CCC: $19.00
Published on Web 08/12/2000

kinases thus regulate their different autophosphorylation states in vivo, and may therefore also direct their different cellular roles.

EXPERIMENTAL PROCEDURES

Expression Vectors. The construction of the plasmids used in this study has been previously described (*11*). Influenza hemaglutinin (HA)-tagged $p94^{fer}$ and $p51^{ferT}$ and their variants: ferΔ1−148, ferΔ1−299, ferΔ1−315, ferΔ1−376, ferΔ124−375, ferΔ331−421, ferΔ330−515, ferΔ685−756, ferΔ816−823, ferΔ1−427, and ferTΔ446−453, were expressed from the pECE vector under the control of the SV40 early promoter. Nontagged $p94^{fer}$ was also expressed from the pECE vector (*11*).

For constructing the HA-tagged ferΔ453−823: nt 970−1428 of the murine fer cDNA were amplified by PCR using the forward primer GGGTTAACAGCAGACGTTTG and the reverse primer CGTCTAGACTAACCCACAGAGATCACATC. The PCR product was flanked by *Eag*I and *Xba*I sites and was inserted into a pECEfer plasmid (*11*) that was partially cut with *Eag*I and *Xba*I.

For ecdysone-regulated expression in CHO cells, the pVgRXR plasmid, which directs the expression of the ecdysone receptor, and the pINDHAferΔ453−823 plasmid were used (*18*). The pINDHAferΔ453−823 plasmid was constructed as follows: pECEHAferΔ453−823 was cut with *Eco*RI and *Xba*I, and the FER fragment so obtained was inserted into a pIND (*18*) plasmid which was also cut with *Eco*RI and *Xba*I.

Transient Transfections of Cells. COS1 cells were grown in DMEM supplemented with 10% FCS. For transfection, 5×10^5 cells were mixed with 8 μg of DNA together with 35 μL of Lipofectamine (Life Technologies, Inc.) in 100 mm dishes for approximately 6 h. During transfection the cells were grown in OPTIMEM medium (Life Technologies, Inc.). The medium was then replaced with OPTIMEM supplemented with 10% FCS, and the cells were incubated for a further 40 h. For cotransfection experiments, 4 μg of each plasmid was mixed and used for transfections.

CHO and HeLa cells were transiently transfected using the cationic lipid RPR120535 (*19*). Cells were grown in DMEM supplemented with 10% FCS. For transfection, 8 μg of DNA was mixed with 700 μL of 80 μM RPR 120535 for 15 min. The mixture was then added to 5×10^5 cells in DMEM without serum for 2 h. 10% FCS was then added to the cells which were further incubated for approximately 48 h.

Establishment of Stable CHO Clones Expressing the N-Terminal Tail of $p94^{fer}$. For establishing stable CHO clones which express the N-terminal tail of $p94^{fer}$ in an ecdysone-dependent manner, the ecdysone-inducible expression system (EIES) was used (*18*). CHO cells were grown in DMEM supplemented with 10% FCS, and 5×10^5 cells were transfected with 20 μg of pVgRXR vector DNA encoding the ecdysone receptor, using the calcium phosphate precipitation technique (*20*). pVgRXR-expressing cells were selected with 0.75 mg/mL zeocin and were retransfected with the pINDHAferΔ453−823 expression vector. Cells expressing both the ecdysone receptor and the $p94^{fer}$ N-terminal tail were double-selected with 0.4 M Geneticin and zeocin. Expression of HA-tagged ferΔ453−823 was induced by treating the cells with 1 μM muristerone A (a synthetic deviate of ecdysone) for 24 h.

Immunoprecipitation. Proteins were extracted from 5×10^5 transfected COS1 cells using tridetergent lysis buffer: 10 mM Tris-HCl (pH 7.5), 150 mM NaCl, 1 mM EDTA, 1% v/v Nonidet P40, 0.5% v/v sodium deoxycholate, 3 mM sodium orthovanadate, 20 μg/mL aprotinin, 20 μg/mL leupeptin, 40 μg/mL Pefablock, and 40 μg/mL benzamidine. The amount of total protein was determined using the Bradford reagent. For each immunoprecipitation, 300 μg of extracted protein was incubated overnight at 4 °C with 1:100 diluted monoclonal αHA (Boehringer), 1:400 diluted monoclonal αPT (UBI), or 1:100 diluted αFER polyclonal antibodies directed against the SH2 domain of $p94^{fer}$. Immunocomplexes were precipitated with protein A Sepharose. Immunoprecipitates were resolved in 8% SDS−PAGE, blotted onto nitrocellulose membrane, and were then reacted with monoclonal αHA antibodies (Babco), with monoclonal αPT antibodies (PT-66, Sigma), with polyclonal αFER C1 antibodies directed against the last 16 aa of the murine $p94^{fer}$ (*20*), or with polyclonal αFER antibodies.

Western Blot Analysis. Proteins were extracted from the transfected COS1 cells using the tridetergent lysis buffer, as above. Protein extract (30 μg) was resolved in 8% SDS−PAGE. Electroblotted proteins were detected by Western blot analysis using monoclonal αHA antibody (Babco), αFER C1 antibodies (*20*), or monoclonal αPT antibody (PT-66, Sigma). Bound monoclonal antibodies were detected with peroxidase-conjugated goat anti-mouse antibody using the chemoluminiscence detection system. Rabbit polyclonal antibodies were detected with peroxidase-conjugated goat anti-rabbit antibody.

Flow-Cytometry Analysis. The transfected CHO and HeLa cells were fixed 48 h post-transfection using 70% ethanol, and blocking was carried out with 2% BSA, and 0.5% Tween 20 for 30 min at 4 °C. The cells were exposed for 1 h to 1:50 diluted αHA monoclonal antibody (Babco) and were subsequently stained with FITC-conjugated donkey anti-mouse antibody. Cells were then treated for 15 min with 5 μg/mL RNase A and stained with 5 μg/mL propidium iodide. Double-stained cells and cells stained with propidium iodide only were separated and analyzed for relative DNA content by a Coulter FACSort (Becton Dickinson) flow cytometer. The different cell cycle populations were determined by the MultiCycle AV application (Phoenix Flow Systems).

RESULTS

N-Terminal Sequences Mediate the in Vivo Oligomerization and the Autophosphorylation of $p94^{fer}$ in-Trans. To explore the role of trans autophosphorylation in the activation of oligomerized $p94^{fer}$ in vivo, $p94^{fer}$ was ectopically coexpressed in COS1 cells together with its HA-tagged, N-terminal tail (Figure 1, ferΔ453−823). To test whether the $p94^{fer}$ N-terminal fragment could associate and oligomerize with the native full-length $p94^{fer}$ in this system, whole cell protein extracts were immunoprecipitated with αHA monoclonal antibody and were then reacted with αFER C1 (*20*) and αHA antibody by a Western blot analysis. αFER C1 antibodies which were directed against the last 16 aa of $p94^{fer}$ (*20*) revealed the coimmunoprecipitation of the overexpressed full-length $p94^{fer}$ together with the HA-tagged N-terminal

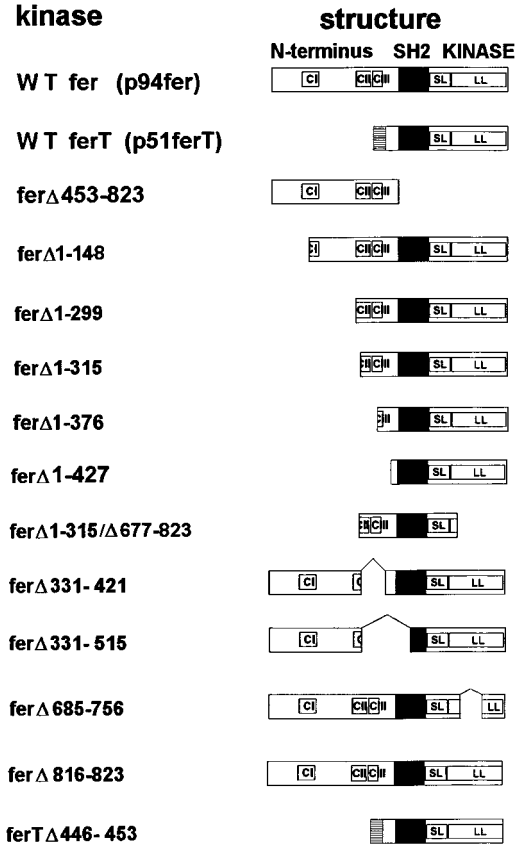

FIGURE 1: Schematic representation of the FER proteins which were studied in this work. Boxed C, CC domains I, II, and III; SL, kinase domain small lobe; LL, kinase domain large lobe. Stippled box in $p51^{ferT}$, the unique NH_2-terminal sequence of the enzyme.

fragment (Figure 2A, lane 2). Moreover, the levels of the precipitated $p94^{fer}$ were comparable to the levels of HA-$p94^{fer}$ which was directly precipitated by the αHA antibody from HA-$p94^{fer}$ expressing cells (Figure 2A, lanes 2 and 5; Figure 2B, lanes 2 and 5). $p94^{fer}$ was not precipitated by the αHA antibody when expressed in the absence of the HA-tagged N-terminal fragment (Figure 2A, lane 1). Thus, as was previously shown (*13*), the N-terminal sequences of $p94^{fer}$ can oligomerize with the full-length kinase in an heterologous co-overexpression system.

To test whether autophosphorylation in-trans is a key step in the activation of oligomerized $p94^{fer}$, the tyrosine phosphorylation state of ectopically expressed and self-oligomerized HA-tagged $p94^{fer}$ was compared to the tyrosine phosphorylation state of $p94^{fer}$ which was coexpressed and oligomerized in vivo with the HA-tagged N-terminal tail (ferΔ453−823). $p94^{fer}$ was immunoprecipitated from the two different preparations using αHA antibody, and was probed with αPT antibody to evaluate its tyrosine phosphorylation state in vivo. Homooligomerized HA-$p94^{fer}$ reacted with the αPT antibody (Figure 2E, lane 5). This phosphorylation most probably reflects the autophosphorylation of $p94^{fer}$ in vivo, since an overexpressed HA-tagged $p94^{fer}$ mutant—Y715F—which lacks the main $p94^{fer}$ autophosphorylation acceptor site (*11*) did not react with the αPT antibody (data not shown).

Unlike the homooligomerized HA-$p94^{fer}$, $p94^{fer}$ co-immunoprecipitated with the HA-tagged N-terminal tail did not exhibit any tyrosine phosphorylation in vivo (Figure 2E, lane 2). Moreover, while whole cell extracts from $p94^{fer}$ and

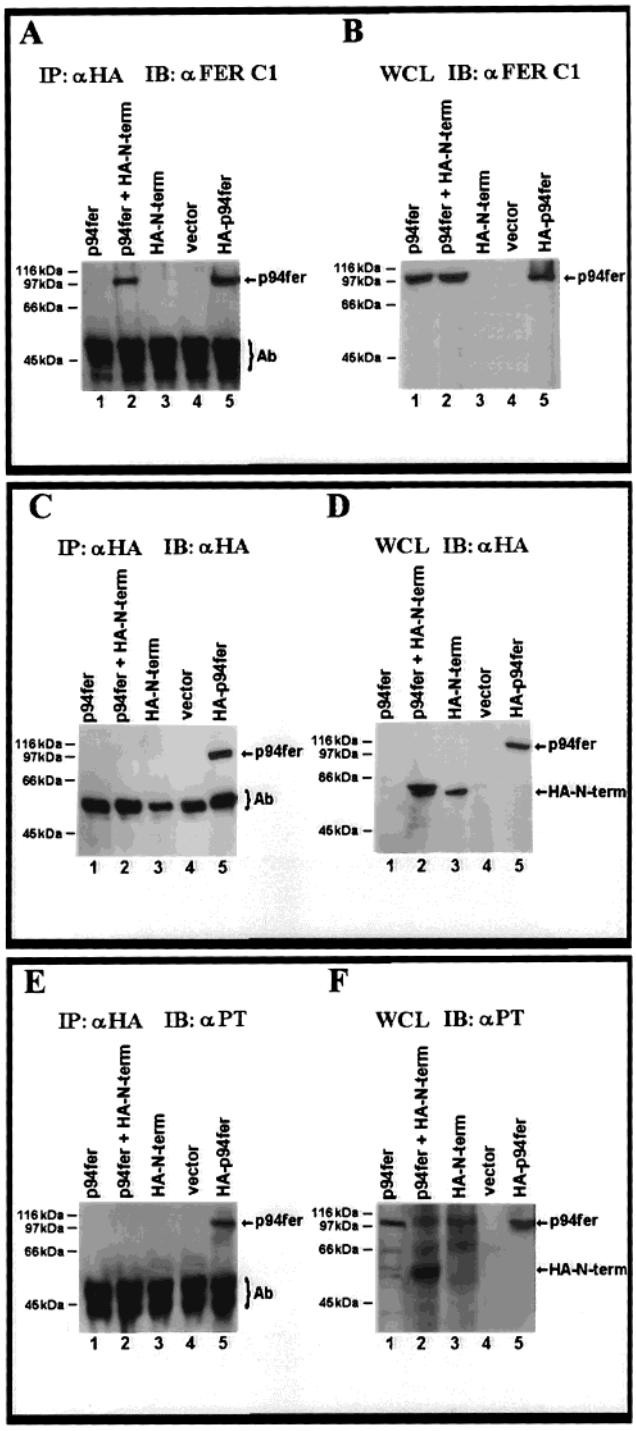

FIGURE 2: N-terminal sequences of $p94^{fer}$ drive the oligomerization and autophosphorylation in-trans of $p94^{fer}$. (A) Whole cell extracts were prepared from COS1 cells transfected with vector expressing $p94^{fer}$ (lane 1), with vector expressing $p94^{fer}$ and the HA-tagged N-terminal tail of $p94^{fer}$ (lane 2), with vector expressing the HA-N-terminal tail alone (lane 3), with the expression vector alone (lane 4), and with vector expressing HA-tagged $p94^{fer}$ (lane 5). HA-tagged proteins were immunoprecipitated with αHA antibody, resolved in 8% SDS−PAGE, and then probed with αFER C1 antibodies. Arrow on the right indicate migration distances of the ectopic $p94^{fer}$. (B) The whole cell extracts as in (A) were resolved by SDS−PAGE and were then probed with αFER C1 antibodies. (C) The αHA immunoprecipitates from (A) were resolved by SDS−PAGE and were then probed with αHA monoclonal antibody. (D) Whole cell extracts as in (A) were resolved in SDS−PAGE and were then probed with αHA antibody. (E) αHA immunoprecipitates from (A) were probed with αPT antibody. (F) Whole cell extracts as in (A) were resolved by SDS−PAGE and were probed with αPT antibody.

HA-tagged p94^{fer} overexpressing cells exhibited a strong tyrosine-phosphorylated 97 kDa band, which most probably corresponds to tyrosine-phosphorylated p94^{fer} (Figure 2F, lanes 1 and 5), no such band was seen in COS1 cells overexpressing both p94^{fer} and the HA-tagged N-terminal tail (Figure 2F, lane 2). This could reflect a preferential formation of hetero-oligomers between the native p94^{fer} kinase and the HA-tagged N-terminal tail, a process which seems to abolish almost completely the autophosphorylation of p94^{fer}. The tyrosine-phosphorylated 97 kDa band was also absent in extracts prepared from cells transfected with the expression vector alone (Figure 2F, lane 4).

The autophosphorylation of oligomerized native p94^{fer} in vivo thus seems to result mainly from reciprocal autophosphorylation in-trans which is carried out among the oligomerized p94^{fer} molecules. Surprisingly, the HA-tagged N-terminal fragment of p94^{fer} became tyrosine-phosphorylated when coexpressed with the native p94^{fer} (Figure 2F, lane 2). This was not seen when the N-terminal fragment was expressed alone (Figure 2E, lane 3), thus indicating that p94^{fer} can trans-phosphorylate the N-terminal fragment, in the hetero-oligomer. Trans-phosphorylation of the HA-tagged N-terminal tail of p94^{fer} by the intact p94^{fer} could not be seen when the truncated fragment was immunoprecipitated with αHA antibody, since in SDS−PAGE it comigrated with the precipitating antibody (Figure 2E, lane 2). The trans-phosphorylation of the N-terminal fragment by p94^{fer} could indicate a bona fide N-terminal p94^{fer} autophosphorylation acceptor site. Alternatively, this phosphorylation may reflect an artificial phosphorylation event which takes place only in the aberrant oligomers which are formed by p94^{fer} and its HA-tagged N-terminal tail. To address this point and to substantiate the fact that autophosphorylation of oligomerized p94^{fer} occurs in-trans, an HA-tagged p94^{fer} inactive deletion mutant which lacks 71 aa of the large lobe in its kinase domain (Figure 1, ferΔ685−756) was coexpressed with a nontagged native p94^{fer} in COS1 cells. ferΔ685−756 also lacks the major autophosphorylation acceptor site of p94^{fer} [Y^{715}, (*12*)]. When this mutant was included in the oligomerization complex of p94^{fer} (Figure 3A, lane 3), it did not react with αPT antibody (Figure 3B, lane 3). Thus, the absence of 71 aa from the kinase domain prevented the trans-phosphorylation of the ferΔ685−756 mutant which still carries the potential N-terminal phosphorylation site. Moreover, the inclusion of the inactive ferΔ685−756 mutant in the hetero-oligomer with intact p94^{fer} interfered with the autophosphorylation of the native enzyme (Figure 3B, lane 3) since the mutant is kinase inactive, and cannot trans-phosphorylate. However, co-oligomerization of p94^{fer} and an inactive p94^{fer} mutant which retains the Y^{715} autophosphorylation site [Figure 1, ferΔ816−823, and (*11*)], but lacks the last 8 carboxy-terminal aa of p94^{fer} (*12*), led to the tyrosine phosphorylation of that mutant (Figure 3B, lane 1). These results confirm that autophosphorylation of oligomerized p94^{fer} in vivo is carried out in-trans. The potential N-terminal autophosphorylation site in p94^{fer} does not seem, however, to be phosphorylated in the context of the intact p94^{fer} enzyme and does not seem therefore to have a physiological significance.

N-Terminal CC Domains Cooperate To Drive the Oligomerization of p94^{fer}. The N-terminal tail of p94^{fer} contains three predicted N-terminal CC domains. These extend from

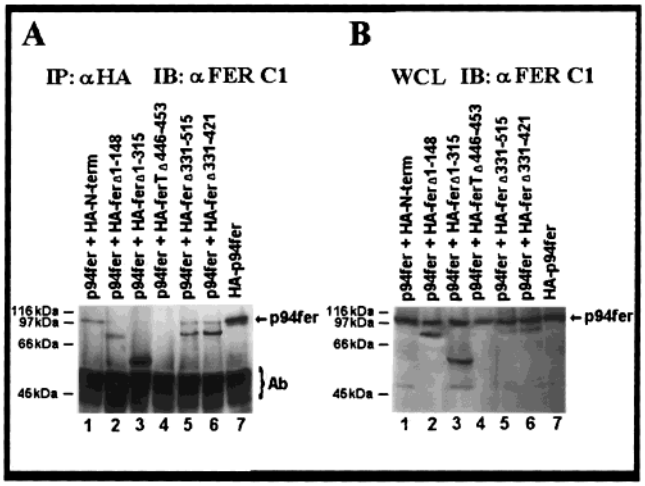

FIGURE 3: Inactive p94^{fer} mutants interfere with the autophosphorylation in-trans of native p94^{fer}. (A) Whole cell extracts were prepared from COS1 cells transfected with plasmids encoding the FER variants (deletion mutants) described on the top of the figure. HA-tagged proteins were immunoprecipitated with αHA antibody, then resolved in 8% SDS−PAGE, and probed with αFER C1 antibodies. Arrows on the right indicate the migration distance of p94^{fer}. The ferΔ816−823 mutant could not be detected with the αFER C1 antibodies since it lacks the last 8 aa of p94^{fer}, which are recognized by the αFER C1 antibodies. (B) The extracts as in (A) were immunoprecipitated with αHA antibody, resolved in SDS−PAGE, and probed with αPT monoclonal antibody.

aa 121−178 (Figure 1, CCI), from aa 301−342 (Figure 1, CCII), and from aa 357−387 (Figure 1, CCIII). To assess the relative contribution of each of these CC domains to the oligomerization of p94^{fer}, the oligomerization potential of various p94^{fer} deletion mutants was analyzed. HA-tagged N-terminal truncated forms of p94^{fer} were expressed in COS1 cells together with the intact enzyme. Whole cell proteins were immunoprecipitated with αHA antibody, and the ability of each truncated p94^{fer} variant to oligomerize with the intact p94^{fer} was determined. Removal of CCI and part of CCII (Figure 1, ferΔ1−315) abolished almost completely the ability of the truncated enzyme to coimmunoprecipitate with the intact enzyme (Figure 4A, lane 3). Similar results were obtained when only 50% of CCI was removed from an HA-tagged p94^{fer} (Figure 1, ferΔ1−148) and (Figure 4A, lane 2). When CCIII and part of CCII (Figure 1, ferΔ331−515 and ferΔ331−421) were removed from the N-terminal region of p94^{fer}, the oligomerization potential of these mutants was reduced but was not completely abolished (Figure 4A, lanes 5 and 6, respectively). Removal of all three CC domains (Figure 1, ferTΔ446−453) completely abolished the ability of the FER proteins to oligomerize (Figure 4A, lane 4). Thus, all three N-terminal CC regions in p94^{fer} cooperate to drive efficient oligomerization of the enzyme. Removal of any of these domains impaired the ability of p94^{fer} to oligomerize. Yet, the relative contribution of CCI seems to be dominant in this oligomerization process, since removal of only 50% of that domain almost completely abolished the oligomerization potential of p94^{fer}.

Ectopically Expressed p94^{fer} N-Terminal Tail Associates with the Endogenous Enzyme in CHO Cells. To substantiate the notion that p94^{fer} oligomerizes in vivo, the ability of an ectopic N-terminal tail of p94^{fer} to associate with the endogenous enzyme was studied in mammalian cells. The HA-tagged, 452 aa long N-terminal tail of p94^{fer} (Figure 1,

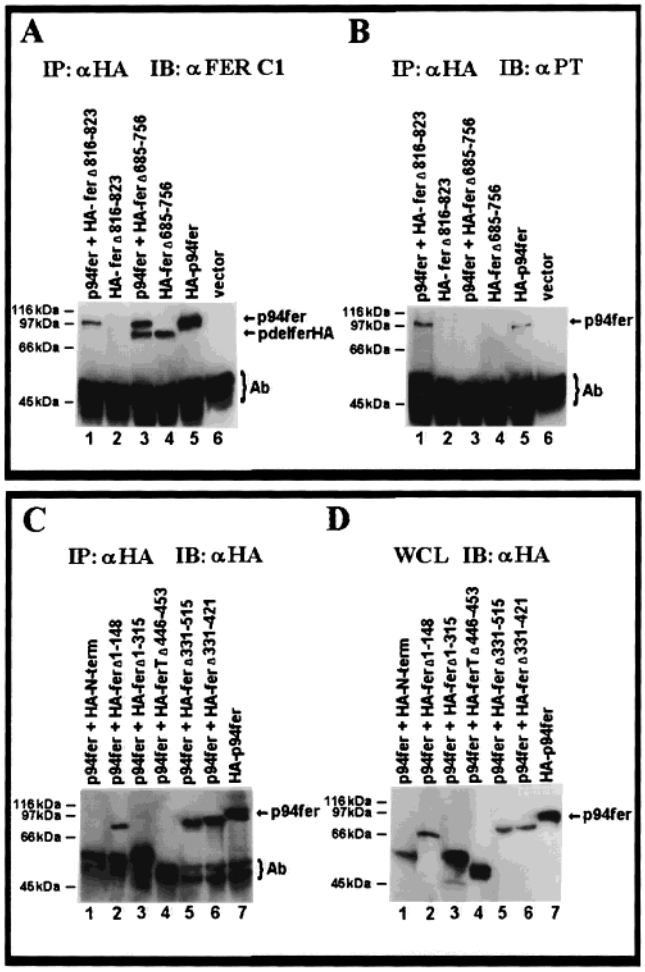

FIGURE 4: N-terminal coiled-coil domains cooperate to drive the oligomerization of p94^{fer}. (A) Whole cell extracts were prepared from COS1 cells transfected with plasmids encoding the FER variants indicated at the top of the figure. HA-tagged proteins were immunoprecipitated using αHA antibody, resolved by SDS−PAGE, and probed with αFER C1 antibodies. Arrows on the right indicate the migration distance of p94^{fer} and of its deletion mutant (pdelferHA). (B) Whole cell extracts from (A) were resolved by 8% SDS−PAGE and were then probed with αFER C1 antibodies using Western blot analysis. (C) HA-tagged proteins were immunoprecipitated with αHA antibody, resolved by SDS−PAGE, and probed with αHA antibody, using Western blot analysis. (D) Whole cell extracts from (A) were resolved in SDS−PAGE and were then probed with αHA antibody, in a Western blot.

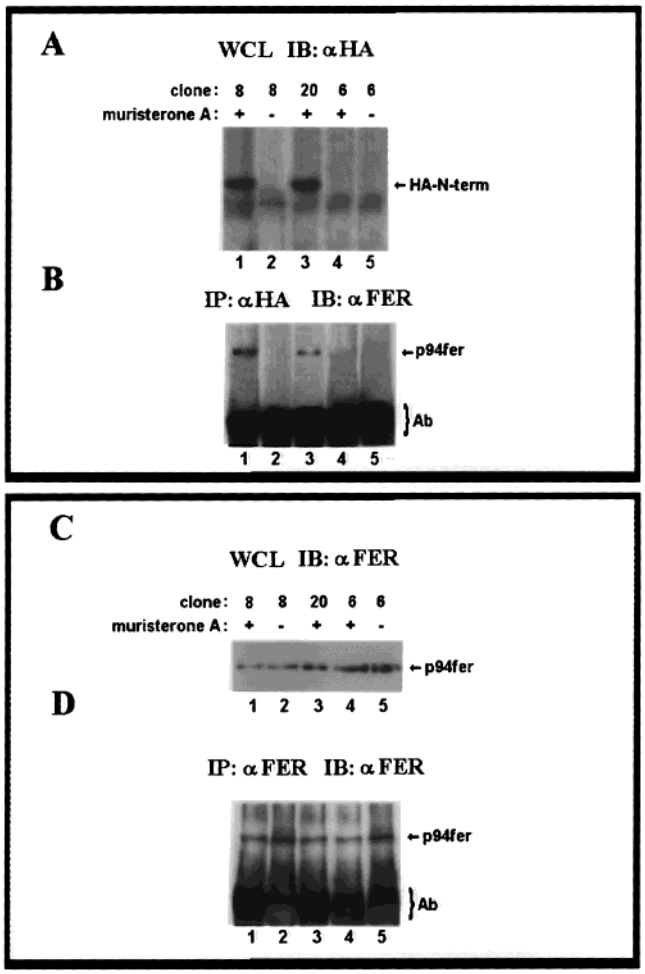

FIGURE 5: Association of the ectopically expressed N-terminal tail of p94^{fer}, with the endogenous p94^{fer}. HA-tagged N-terminal tail of p94^{fer} was expressed in CHO cells under the control of a muristerone A responsive promoter. (A) The levels of the HA-tagged N-terminal tail were determined in whole cell lysates (WCL) prepared from clones transfected (clones 8 and 20) or nontransfected (clone 6) with the N-terminal tail expression vector pINDHA-ferΔ453−823. The proteins were resolved in 9% SDS−PAGE and were detected in Western blot analysis using αHA antibody. Lane 1, clone 8 cells treated with muristerone A; lane 2, untreated clone 8 cells; lane 3, clone 20 cells treated with muristerone A; lanes 4 and 5, treated and untreated clone 6 cells, respectively. Arrow on the right indicates migration distance of HA-tagged N-terminal tail of p94^{fer}. (B) Coimmunoprecipitation of the endogenous p94^{fer} together with the HA-tagged N-terminal tail. The HA-tagged N-terminal tail of p94^{fer} was immunoprecipitated from the same extract described in (A). The precipitated proteins were resolved in 8% SDS−PAGE and were exposed to αFER antibodies, in Western blot analysis. Arrow on the right indicates migration distance of the endogenous CHO p94^{fer}. (C) The whole cell lysates from (A) were probed with αFER antibodies in a Western blot. (D) Endogenous CHO p94^{fer} was immunoprecipitated from the samples described in (A) using αFER antibodies. The precipitated proteins were resolved by 8% SDS−PAGE and then probed with the same αFER antibodies, by Western blot.

ferΔ453−823) was stably expressed in CHO cells under the control of a modified ecdysone responsive promoter (*18*). Several clones expressing both the ecdysone receptor and the N-terminal tail of p94^{fer} were isolated and further analyzed. Exposing these clones to the synthetic analogue of ecdysone, muristerone A, led to the accumulation of the HA-tagged 50 kDa N-terminal tail of p94^{fer} in the transfected cells (Figure 5A, lanes 1−3). No protein of that size was detected by the αHA antibody in the parental cell line, which expressed only the ecdysone receptor (Figure 5A, lanes 4, 5). To test the association of the N-terminal fragment of p94^{fer} with the endogenous kinase, coimmunoprecipitation experiments of the endogenous p94^{fer} and the ectopic N-terminal tail were performed. Immunoprecipitation of the HA-tagged p94^{fer} N-terminal fragment with αHA antibody led to the coprecipitation of the endogenous p94^{fer}. Moreover, the levels of p94^{fer} which coprecipitated with the N-terminal tail were comparable to those precipitated directly by αFER antibodies (compare Figure 5B and Figure 5D).

This was seen only in extracts prepared from cells which were induced to produce the ectopic N-terminal p94^{fer} tail (Figure 5B, lanes 1−3). No signal was seen in αHA precipitates prepared from the parental cells which harbored the ecdysone receptor alone (Figure 5B, lanes 4, 5) or in transfected cells which were not induced with muristerone

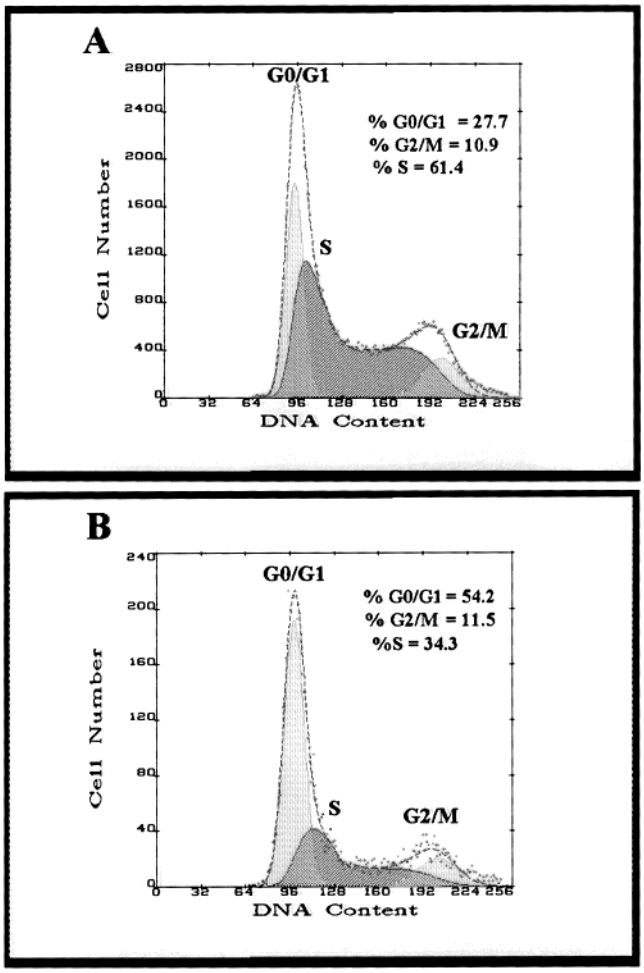

FIGURE 6: Cell cycle profiles of cells expressing native and dominant negative mutants of p94^{fer}. (A) Untransfected CHO cells stained with propidium iodide and analyzed by a FACSort flow cytometer. (B) CHO cell overexpressing the N-terminal tail of p94^{fer} (ferΔ453−823HA) double stained with αHA and propidium iodide and analyzed by a FACSort flow cytometer. The different shadings represent the G0/G1, S, and G2/M populations, respectively, as defined by the MultiCycle AV application (Phoenix Flow Systems). The percentages given in the right top corner of the figure were obtained in one out of three independent experiments, which gave similar results.

A. These experiments clearly demonstrate that N-terminal sequences mediate the oligomerization of p94^{fer} in vivo.

Overexpressed N-Terminal Sequences of p94^{fer} Increase the Percentage of G0/G1 Cells. The association of an ectopically expressed N-terminal tail of p94^{fer} with the endogenous enzyme enables one to use that fragment as a dominant negative mutant of p94^{fer}. This could serve as an efficient tool for studying the cellular role of p94^{fer}. The p94^{fer}-derived fragment which carries the N-terminal 452 aa of the enzyme (Figure 1, ferΔ453−823) was transiently overexpressed in CHO and HeLa cells. Cells expressing the HA-tagged N-terminal fragment were selected using a flow cytometer, and their cell-cycle profile was compared to that of nonexpressing cells. While about 25% of the nontransfected cells reside in the G0/G1 phase, 50% of the cells expressing the N-terminal tail of p94^{fer} were found to reside in that phase (Figure 6 and Table 1). This increase in the percentage of G0/G1 cells was accompanied by a significant reduction in the percentage of cells residing in the S phase (Figure 6 and Table 1). A similar effect was seen in cells

Table 1: Cell Cycle Profiles of CHO and HeLa Cells Expressing Native and Dominant Negative Mutant of p94^{fer} [a]

cell type	FER	G0/G1 (%)	S (%)	G2M (%)
CHO	−	28	61	10
	N-terminus	55	32	14
	p94^{fer}	35	60	6
	ferΔ1−315/Δ677−823	26	63	11
HeLa	−	25	60	15
	N-terminus	46	44	10
	p94^{fer}	27	67	7

[a] Nontransfected cells and cells overexpressing the N-terminal tail of p94^{fer} or the native enzyme were subjected to flow-cytometry analysis. The percentage of cells in each of the stages of the cell cycle are shown. These experiments were repeated 3 times and gave similar results.

expressing a nonactive mutant of p94^{fer} which carries an inactivating deletion in its kinase domain (data not shown). However, unlike the inactive mutants, overexpression of the native p94^{fer} did not lead to a significant change in the percentage of G0/G1 cells but rather decreased the percentage of G2/M cells (Table 1). Similarly, an N-terminal construct devoid of CC domain I and 38% of CC domain II (Figure 1, ferΔ1−315/Δ677−823) also failed to increase the G0/G1 population (Table 1, ferΔ1−315/Δ677−823), in CHO cells. Thus, the increase in G0/G1 cells is specifically caused by defined sequences in the p94^{fer} N-terminal tail.

Unique N-Terminal Sequences of p51^{ferT} Interfere with Its Autophosphorylation Activity in Vivo. p51^{ferT} lacks N-terminal CC domains (Figure 1), a fact which could explain its inability to oligomerize (Figure 4A, lane 4); we next studied, therefore, the autophosphorylation of p51^{ferT} in vivo. The tyrosine phosphorylation of p51^{ferT} was compared to the tyrosine phosphorylation profile of four p94^{fer} N-terminal truncation mutants. Like p51^{ferT}, these mutants fail to oligomerize in vivo, and they reside constitutively in the cell nucleus (*11*). COS1 cells were transfected with HA-tagged ferΔ1−299 which lacks CCI (Figure 1) and which does not oligomerize in vivo (data not shown), ferΔ1−315 which lacks CCI and part of CCII (Figure 1), ferΔ1−376 which lacks CCI, CCII, and most of CCIII (Figure 1), and ferΔ1−427 which lacks all three CC domains (Figure 1). All FER variants were efficiently expressed in the transfected cells (Figure 7B). Since some of these truncated forms of p94^{fer} migrate similarly to the light chains of the precipitating antibodies in SDS−PAGE, their in vivo tyrosine phosphorylation states were determined using both immunoprecipitation (Figure 7A) and Western blot analysis of whole cell extracts, using αPT antibody (Figure 7C). Tyrosine-phosphorylated variants were immunoprecipitated from COS1 expressing cells, using αPT antibody, and were then detected using αHA antibody. This enabled us to specifically precipitate and detect the tyrosine-phosphorylated fraction of each of the different FER variants. Reacting the αPT immunoprecipitates with αHA antibody revealed the tyrosine phosphorylation of ferΔ1−299 and ferΔ1−315 in vivo (Figure 7A, lanes 1 and 2, marked with pdelferHA on the left side of the figure).

Surprisingly, in cells overexpressing p51^{ferT}, no obvious band of the correct size of p51^{ferT} was detected which specifically reacted with the αHA antibody (Figure 7A, lane 4) following immunoprecipitation with αPT, and the reaction

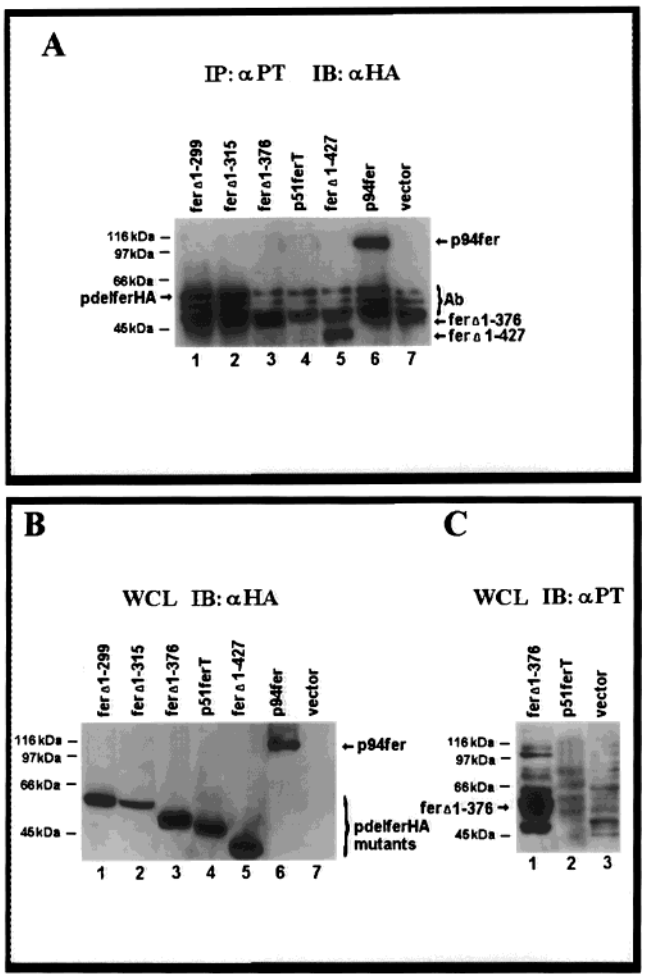

FIGURE 7: N-terminal sequences interfere with the autophosphorylation of $p51^{ferT}$. (A) Whole cell extracts were prepared from COS1 cells transfected with the FER variants which are listed at the top of the figure. Tyrosine-phosphorylated proteins were immunoprecipitated with αPT monoclonal antibody. The precipitated proteins were resolved by 10% SDS−PAGE and were then probed with αHA in a Western blot. Migration distances of tyrosine-phosphorylated FER variants are indicated. pdelferHA (marked by an arrow on the left side of the figure) indicated the migration distance of phosphorylated ferΔ1−299 and ferΔ1−315. Migration distances of phosphorylated ferΔ1−376 and ferΔ1−427 are marked by arrows on the right side of the figure. (B) Whole cell extracts as in (A) were probed with αHA in a Western blot analysis. Migration distances of $p94^{fer}$ and its deletion mutants (delferHA) are marked on the right side of the figure. (C) Whole cell extracts from cells transfected with vector expressing ferΔ1−376 (lane 1) and $p51^{ferT}$ (lane 2) and from cells transfected with the parental vector alone (lane 3) were probed with αPT antibody in a Western blot. The migration distance of the tyrosine-phosphorylated ferΔ1−376 is indicated on the left.

pattern was similar to that obtained from COS1 cells transfected with the expression vector alone (Figure 7A, lane 7). In accordance with that, no obvious band which could correspond to $p51^{ferT}$ was detected by the αPT antibody in Western blot analysis of whole cells extracts prepared from $p51^{ferT}$-expressing cells or from cells transfected with the expression vector alone (Figure 7C, lanes 2 and 3, respectively). However, removal of the unique N-terminal tail of $p51^{ferT}$ (Figure 1, ferΔ1−427) led to the tyrosine phosphorylation of this FER variant in vivo and to its precipitation by the αPT antibody (Figure 7A, lane 5). Similarly, replacing the unique N-terminal 43 aa of $p51^{ferT}$ with the parallel 36 aa from the N-terminal tail of $p94^{fer}$ (Figure 1, ferΔ1−376) endowed the modified $p51^{ferT}$ with the ability to autophosphorylate in vivo (Figure 7A, lane 3). Thus, a prominent 50 kDa tyrosine-phosphorylated protein which corresponds to ferΔ1−376 could also be detected by the αPT antibody in whole cell extracts prepared from ferΔ1−376 expressing cells. These results suggest that the unique N-terminal 43 aa in $p51^{ferT}$ impair its ability to autophosphorylate in vivo.

DISCUSSION

$p94^{fer}$ and $p51^{ferT}$ are two highly related tyrosine kinases which share identical SH2 and kinase domains but differ in their N-terminal tails. We have previously shown that the extended N-terminal tail of $p94^{fer}$ controls the subcellular localization profile of $p94^{fer}$, which differs from the one exhibited by $p51^{ferT}$ (*11*). Three CC-forming domains were shown to be involved in controlling the subcellular localization of $p94^{fer}$ (*11*). Recently, it was shown that the N-terminal CC domains in $p94^{fer}$ can also drive the trimerization of the enzyme (*13*). Similarly, N-terminal CC regions in the Fer-related kinase, c-fes, were also shown to mediate its oligomerization in vivo (*14*).

In the current study, we showed that ectopically expressed $p94^{fer}$ fragment which carries the N-terminal tail of the kinase can associate with the endogenous enzyme (Figure 5). This substantiates the relevance of the oligomerization of $p94^{fer}$ in vivo. We have therefore examined the role of the $p94^{fer}$ N-terminal oligomerization domains in mediating the autophosphorylation of that kinase, in vivo. We show here that $p94^{fer}$ undergoes autophosphorylation in-trans in vivo and that oligomerization mediates this process. Co-oligomerization of an inactive and an intact $p94^{fer}$ kinase significantly interfered with the autophosphorylation of the native $p94^{fer}$ (Figures 2 and 3). Interestingly, however, oligomerization is not required for the autophosphorylation of the FER kinases, since truncated variants of $p94^{fer}$ which failed to oligomerize still exhibited prominent autophosphorylation activity [(*13*) and Figure 7]. This may reflect a deregulated autophosphorylation activity of the truncated FER variants which could occur in vivo in-cis. The occurrence of native $p94^{fer}$ in high molecular weight complexes in the cell (*12*) may also suggests that the activation of the native enzyme in vivo is carried out through the autophosphorylation in-trans process. However, the N-terminal tail of $p94^{fer}$ does not only drive the oligomerization of the kinase but also mediates its interaction with cell−cell adhesion molecules, such as p120CAS (*12*). Growth factor stimulation of cells may change the composition of the $p94^{fer}$-associated complexes, thus allowing the oligomerization and autophosphorylation of $p94^{fer}$ in-trans (*12*). Thus, although the N-terminal tail of $p94^{fer}$ is not essential for the autophosphorylation of the enzyme, it may impose controls that could restrict the activity of $p94^{fer}$ to certain stages of the cell cycle or to certain subcellular compartments. The role of the N-terminal tail of $p94^{fer}$ in mediating the oligomerization and activation of that kinase turns a fragment which carries these sequences into a potential dominant negative mutant. Overexpression of such a fragment in CHO and HeLa cells markedly increased the percentage of cells which reside in the G0/G1 phase. A similar effect was caused by a nonactive $p94^{fer}$ mutant (data not shown), but it was not seen in cells overexpressing the intact $p94^{fer}$ (Figure 6). The N-terminal tail

of p94^{fer} could affect the progression of the G1 phase by binding to cell cycle regulatory proteins such as β-catenin which was shown to associate with p94^{fer} (*16*). To exclude that possibility, we verified the fact that β-catenin does not bind to the N-terminal tail of p94^{fer} (Halachmi-Priel, S., and Nir, U., unpublished data). These results substantiate the specificity of the observed cellular effect and suggest a role for p94^{fer} in regulation of G1 progression or in the transition of cells from G1 to S phase. Similar to p94^{fer}, the N-terminal tail of c-fes was also shown to exert a dominant negative activity, and it interfered with the transforming activity of c-fes (*21*). It is unlikely, however, that the cellular effect caused by the N-terminal tail of p94^{fer} results from its cross-association with the endogenous c-fes since the N-terminal tails of these two related kinases do not form heterotypic oligomers (*11*). It should also be noted that while the CCI domain in c-fes exerts a negative effect on the kinase activity (*21*), the CCI domain of p94^{fer} plays a pivotal positive role in the oligomerization and autophosphorylation of the native enzyme in vivo. Thus, despite the similar structure of the two related kinases, their activity is regulated differently.

Few cytoplasmic tyrosine kinases have been shown to oligomerize; thus, p94^{fer} and c-fes are relatively unusual examples. It should be noted, however, that several serine/threonine kinases bear N-terminal CC domains and have been shown to oligomerize in vivo (*22*−*24*).

Unlike p94^{fer}, the meiotic FER variant, p51^{ferT}, does not oligomerize, and is not autophosphorylated in vivo (or is phosphorylated at a relatively low level) (Figure 7). This does not result simply from the inability of p51^{ferT} to oligomerize in vivo, since truncated forms of p94^{fer} which failed to oligomerize did nevertheless exhibit prominent autophosphorylation activity (Figure 7). Deleting the unique N-terminal 43 aa of p51^{ferT}, or replacing it with a parallel N-terminal segment from p94^{fer}, endowed p51^{ferT} with the ability to autophosphorylate (Figure 7). The unique N-terminal tail of p51^{ferT} seems to therefore impose a defined structure on p51^{ferT} in vivo, which prevents its autophosphorylation. Yet p51^{ferT} induces the tyrosine phosphorylation of several nuclear proteins in COS1 cells (Halachmi- Priel, S., and Nir, U., data not shown), indicating that the N-terminal tail of p51^{ferT} does not repress the activity of that enzyme but rather directs it toward a defined specificity. The unique effect of the N-terminal tail of p51^{ferT} does not seem to be mediated through increased susceptibility of the enzyme to mammalian phospho-tyrosine phosphatases since the same differences between the autophosphorylation profiles of p94^{fer} and p51^{ferT} were seen when the two enzymes were ectopically expressed in the yeast *Saccharomyces cerevisiae* (Schwarz, Y., and Nir, U., unpublished results).

The FER tyrosine kinases are therefore two highly related tyrosine kinases whose different N-terminal tails direct their different autophosphorylation profiles and consequently may dictate their different cellular roles.

ACKNOWLEDGMENT

We thank U. Caro for running the flow cytometry analysis, Dr. Gerardo Byk for the cationic lipid RPR120535, and Mrs. S. Kantor for typing the manuscript.

REFERENCES

1. Pawson, T., Letwin, K., Lee, T., Hao, Q.-L., Heisterkamp, N., and Groffen, J. (1989) *Mol. Cell. Biol. 9*, 5722−5725.
2. Paulson, R., Jackson, J., Immergluck, K., and Bishop, J. M. (1997) *Oncogene 14*, 641−652.
3. Hao, Q.-L., Heisterkamp, N., and Groffen, J. (1989) *Mol. Cell. Biol. 9*, 1587−1593.
4. Fischman, K., Edman, J. C., Shackleford, G. M., Turner, J. A., Rutter, W. J., and Nir, U. (1990) *Mol. Cell. Biol. 10*, 146−153.
5. Letwin, K., Yee, S.-P., and Pawson, T. (1988) *Oncogene 3*, 621−627.
6. Roebroek, A. J. M., Schalken, J. A., Verbeek, J. S., Van der Ouweland, A. M. W., Onnekink, C., Bloemers, H. P. J., and Van de Ven, W. J. M. (1985) *EMBO J. 4*, 2897−2903.
7. Keshet, E., Itin, A., Fischman, K., and Nir, U. (1990) *Mol. Cell. Biol. 10*, 5021−5025.
8. Hazan, B., Bern, O., Carmel, M., Lejbkowicz, F., Goldstein, R. S., and Nir, U. (1993) *Cell Growth Differ. 4*, 443−449.
9. Wilks, A. F., and Kurban, R. R. (1988) *Oncogene 3*, 289−294.
10. Yates, K. E., Lynch, M. R., Wong, S. G., Slamon, D. J., and Gasson, J. C. (1995) *Oncogene 10*, 1239−1242.
11. Ben-Dor, I., Bern, O., Tennenbaum, T., and Nir, U. (1999) *Cell Growth Differ. 10*, 113−129.
12. Kim, L., and Wong, T. W. (1995) *Mol. Cell. Biol. 15*, 4553−4561.
13. Craig, A. W., Zirngibl, R., and Greer, P. (1999) *J. Biol. Chem. 274*, 19934−19942.
14. Read, R. D., Lionberger, J. M., and Smithgall, T. E. (1997) *J. Biol. Chem. 272*, 18498−18503.
15. Weiss, A., and Schlessinger, J. (1998) *Cell 94*, 277−280.
16. Rosato, R., Vetmaat, J. M., Groffen, J. and Heisterkamp, N. (1998) *Mol. Cell Biol. 18*, 5762.
17. Penhallow, R. C., Class, K., Sonoda, H., Bolen, J. B., and Rowley, R. B. (1995) *J. Biol. Chem. 270*, 23362−23365.
18. No, D., Yao, T. P., and Evans, R. M. (1996) *Proc. Natl. Acad. Sci. U.S.A. 93*, 3346−3351.
19. Escriou, V., Ciolina, C., Lacroix, F., Byk, G., Scherman, D., and Wils, P. (1998) *Biochim. Biophys. Acta 1368*, 276−288.
20. Bern, O., Hazan, B., and Nir, U. (1997) *FEBS Lett. 403*, 45−50.
21. Cheng, H., Rogers, J. A., Dunham, N. A., and Smithgall, T. E. (1999) *Mol. Cell. Biol. 19*, 8335−8343.
22. Matsui, T., Amano, M., Yamamoto, T., Chihara, K., Nakafuku, M., Ito, M., Nakano, T., Okawa, K., Iwamatsu, A., and Kaibuchi, K. (1996) *EMBO J. 15*, 2208−2216.
23. Roe, J. L., Durfee, T., Zupan, J. R., Repetti, P. P., McLean, B. G., and Zambryski, P. C. (1997) *J. Biol. Chem. 272*, 5838−5845.
24. Futey, L. M., Medley, Q. G., Cote, G. P., and Egelhoff, T. T. (1995) *J. Biol. Chem. 270*, 523−529.

BI0005153